# Stability assessment of organic sulfur and organosulfate compounds in filter samples for quantification by Fourier Transform-Infrared Spectroscopy

Marife B. Anunciado[1], Miranda De Boskey[2], Laura Haines[2], Katarina Lindskog[2], Tracy Dombek[2], Satoshi Takahama[3], Ann M. Dillner[1]

[1]Air Quality Research Center, University of California Davis, Davis, California, United States

[2]Research Triangle Institute, Research Triangle Park, North Carolina, United States

[3]Laboratory of Atmospheric Processes and their Impacts (LAPI), ENAC/IIE, Ecole Polytechnique Fédérale de Lausanne (EPFL), Switzerland

*Correspondence to*: Ann M. Dillner (amdillner@ucdavis.edu)

**Abstract.** Organic sulfur and sulfate compounds, tracers for sources and atmospheric processes, are not currently measured in national monitoring networks such as the Interagency Monitoring of Protected Visual Environments (IMPROVE). The goal of this paper is to begin to assess the stability of organic sulfur and sulfate containing compounds on polytetrafluoroethylene (PTFE) filters and the suitability of Fourier-transform infrared (FT-IR) spectroscopy to measure these compounds. Stability assessment is needed because PTFE samples collected by IMPROVE are typically stored 6-9 months prior to analysis. For this study, two organosulfur compounds, methanesulfonic acid (MSA) and hydroxymethanesulfonate ion (HMS), and two organosulfate compounds, methyl sulfate (MS) and 2-methyltetrol sulfate (2-MTS), are collected individually on PTFE filters. Gravimetric mass measurements are used to assess mass stability over time. FT-IR spectra are evaluated to assess the capability of measuring the compound from PTFE filters by

assessing the compound stability or chemical changes over time. Ion chromatography (IC) and

Inductively Coupled Plasma Optical Emission Spectroscopy (ICP-OES) are used as an additional

tool to assess stability or chemical changes over time. MS has the highest potential to be measured

by FT-IR in IMPROVE samples. For MS, a simple organosulfate, the mass changes are within

measurement uncertainty and FT-IR spectra indicate no compositional change over a 4-month

period, suggesting MS can be measured using FT-IR. IC and ICP-OES support the conclusion

that MS is stable on the filter. However, for 2-MTS, the other organosulfate measured in this study,

spectral changes after a month on the filter suggests it decomposes into other organosulfates or an

inorganic sulfate. MSA in IMPROVE samples can be measured, but only as a lower bound, due

to volatility off of the filter as indicated by FT-IR and gravimetry. FT-IR and IC both show that

MSA is not chemically changing over the course of the study. Measurements by all methods

indicate HMS is unstable on PTFE filter and IC and FT-IR indicate that it likely converts to

inorganic sulfate. Future work includes the evaluation of these compounds in as ambient aerosol

sample matrix to determine any differences in stability, identifying interferences that could limit

quantification and developing calibrations to measure the compounds or functional groups in

ambient samples.

## 1 Introduction

Organic sulfur compounds exist in particulate form in the atmosphere and can be the result of

natural processes (e.g. marine sulfur, volcanic emissions) (Aneja and Cooper, 1989; Bates et al.,

1992) or activities of anthropogenic sources (e.g. combustion, sulfur-rich wastewaters, smelting)

(Grübler, 1998; Smith et al., 2011). Organic sulfur compounds can be categorized as

organosulfur compounds such as sulfones ($RSO_2$) and sulfonic acids ($RSO_3^-$) having C-S bonds,

while organosulfates ($ROSO_3^-$) have a C-O-S bond in the structure (Song et al., 2019). Two

45    sulfonic acid compounds, methanesulfonic acid (MSA), a tracer for marine aerosol, and

46    hydroxymethanesulfonate ion (HMS), measured in high haze conditions, along with two

47    organosulfates compounds, methyl sulfate (MS) and 2-methyltetrol sulfate (2-MTS) were

48    selected for evaluation.

49    Methanesulfonic acid forms from photochemical oxidation of dimethyl sulfide (DMS) (von

50    Glasow and Crutzen, 2004; Kwong et al., 2018a).  DMS is a naturally occurring sulfur species

51    produced by marine algae or phytoplankton and is an important precursor of sulfur dioxide, non-

52    sea salt inorganic sulfate and organosulfur compounds, including MSA (Barnes et al., 1994;

53    Hoffmann et al., 2016).  This makes MSA a tracer for marine aerosol (Allen et al., 1997; Becagli

54    et al., 2013; Saltzman et al., 1986). Ion chromatography (IC) has been used to measure MSA in

55    ambient aerosol collected on PTFE filters (Amore et al., 2022) and nucleopore filters (Allen et

56    al., 2002).  MSA has also been measured in water soluble fractions of ambient aerosol using

57    proton nuclear magnetic resonance (HNMR) (Decesari et al., 2000). Fourier-transform infrared

58    spectroscopy (FT-IR) has been used to characterize liquid and solid MSA in the laboratory

59    studies (Lee et al., 2019; Zhong and Parker, 2022; Chackalackal and Stafford, 1966) as has

60    Raman spectroscopy (Zhong and Parker, 2022), but to the best of our knowledge, neither FT-IR

61    or Raman spectroscopy have been used to measure MSA in complex mixtures like ambient

62    aerosol samples.

63    Hydroxymethanesulfonate (HMS), formed by sulfite and formaldehyde in aqueous phase, is a

64    strong acid that is stable at low pH (Seinfeld and Pandis, 2016) and is a tracer for aqueous

65    processes (Chen et al., 2022).  During severe winter haze in the North China Plain, HMS was

66    measured using real-time single particle mass spectrum instruments and filter-based IC methods

67    during periods of high $SO_2$ and HCHO concentrations and low oxidant concentrations in

68    particles with high liquid water content (Ma et al., 2020).  Very high concentrations of HMS

69    have been measured in Fairbanks, Alaska during pollution events in a cold, dark and humid

70    environment (Campbell et al., 2022). In the Interagency Monitoring of Protected Visual

71    Environments (IMPROVE) Network, there is evidence of an ubiquitous presence of HMS in ion

72    chromatograms of samples collected at 150 sites in the United States (Moch et al., 2020).

73         However, HMS can be challenging to measure (Moch et al., 2018).  Single particle mass

74    spectrometry techniques have identified m/z 111 as characteristic for HMS (Chapman et al.,

75    1990; Lee et al., 2003; Song et al., 2019).  However, methyl sulfate and other organic sulfur

76    compounds have the same characteristic m/z which makes quantifying HMS using mass

77    spectrometry challenging (Dovrou et al., 2019; Lee et al., 2003). High-resolution aerosol mass

78    spectrometry (HR-AMS) has been used to measure HMS and organosulfates, however the

79    majority of compounds  mostly fragment into inorganic sulfate and a non-sulfur containing

80    organic fraction, leading to an underestimation of HMS and overestimation of inorganic sulfate

81    (Dovrou et al., 2019; Song et al., 2019).  HMS has been measured in field and laboratory studies

82    by IC (Dovrou et al., 2019; Campbell et al., 2022), however notable challenges have been

83    documented. HMS and sulfate are not fully resolved in all IC methods (Campbell et al., 2022)

84    leading to poor resolution that can introduce error into the results for both HMS and sulfate

85    (Dovrou et al., 2019; Ma et al., 2020). In IC methods where HMS and sulfate are well resolved,

86    HMS and sulfite may be unresolved and co-elute with bisulfite  (Moch et al., 2018; Wei et al.,

87    2020). Additionally, HMS may degrade to sulfite and formaldehyde at the high-pH eluent used

88    in IC (Moch et al., 2020). Degradation of both HMS and sulfite may occur in aqueous solutions

89    prior to analysis or in the column during analysis and it's suspected that some of the sulfite

90    oxidizes to sulfate in solution or in the column (Moch et al., 2020).  The formation of HMS in

91    the atmosphere occurs at moderate pH and pH differences, between the filter and atmospheric

92    condition (e.g. cloud, fog, pH), can contribute to HMS sample mass loss off the filter leading to

93    an underestimation of HMS (Moch et al., 2020). With proper columns and eluent composition,

94    IC has been shown to separate HMS and sulfate peaks with only a small underestimation of

95    HMS due to sulfate conversion (Dovrou et al., 2019; Campbell et al., 2022).  At least one

96    laboratory study (published in Japanese) has characterized HMS by FT-IR (Sato et al., 1984) but

97    FT-IR has not been used to measure HMS in ambient aerosol samples to the best of our

98    knowledge.

99    Organosulfates are the most abundant form of organic sulfur compounds in atmospheric particles

100   (Hettiyadura et al., 2015; Stone et al., 2012; Hawkins et al., 2010; Frossard et al., 2011; Olson et

101   al., 2011).  Organosulfates are secondary organic aerosols (SOA) from oxidation of mostly

102   biogenic, but also some anthropogenic volatile organic compounds, in the presence of acidic

103   sulfate (Hettiyadura et al., 2015; Stone et al., 2012; Wang et al., 2021) and have been suggested

104   to be tracers for SOA (Wang et al., 2021; Chen et al., 2021). Organosulfates have been measured

105   in ambient aerosol globally including at four sites in Asia where on average they contribute <1%

106   of $PM_{2.5}$, 2.3% of organic carbon and 3.8% of total sulfate (Stone et al., 2012). In Arctic haze

107   aerosols in the spring, organosulfates contributed to 13% of organic matter (OM) (Hansen et al.,

108   2014) and contributed to OM at varying levels across the US, with higher levels in summer

109   (Chen et al., 2021).  Most studies have used a liquid chromatography method coupled to a mass

110   spectrometer (LC-MS) for measuring organosulfates (Hettiyadura et al., 2015; Wang et al.,

111   2021). FT-IR has been used to measure total organosulfate functional groups (Hawkins et al.,

112   2010) and Raman (Lloyd and Dodgson, 1961; Bondy et al., 2018) and FT-IR (Lloyd et al., 1961)

113   have been utilized to characterize organosulfates in laboratory studies.  FT-IR has been used to

114    measure the organosulfate functional group using peak fitting and showed that the organosulfate

115    functional group contributes up to 10% of organosulfate in the Arctic region, when inorganic

116    sulfate concentrations are considered high (Frossard et al., 2011), and 4-8% of OM in the Pacific

117    marine boundary layer, during periods of high organic and sulfate concentrations (Hawkins et al.,

118    2010). While other studies showed little to no organosulfates, likely due to low sulfate

119    concentrations in Mexico City (Liu et al., 2009) and Bakersfield, CA (Liu et al., 2012).

120         Methyl sulfate is the smallest organosulfate (Kwong et al., 2018b) and measured mostly

121    in trace amounts (Hettiyadura et al., 2017, 2015; Wang et al., 2021). However, it is commercially

122    available and therefore useful for laboratory studies.  2-Methyltetrol sulfates are tracers for

123    secondary organic aerosols (SOA) formation in atmospheric particles derived from isoprene

124    (Surratt et al., 2010; Chen et al., 2020) and one of the most abundant organosulfates measured in

125    ambient aerosol. In the eastern US, 2-MTS accounts for the highest percentage summertime

126    particulate organosulfate (11%) (Chen et al., 2021). In Centreville, AL, 2-MTS accounts for

127    more than half of organosulfates during summer of 2013 (Hettiyadura et al., 2017). In Shanghai,

128    China (summer of 2015-2016, 2018-2019), 2-MTS was the most abundant organosulfate (31%)

129    of 29 organosulfates (Wang et al., 2021).

130         The IMPROVE network is a rural particulate matter monitoring network with ~165 sites

131    across the United States (http://vista.cira.colostate.edu/improve/).  Polytetrafluoroethylene

132    (PTFE), nylon and quartz filters are used to collect $PM_{2.5}$ every one in three days, have a field

133    latency period of up to 7 days and are analyzed by multiple analytical techniques.  PTFE filters

134    are stored at room temperature and analyzed between 3 and 12 months after collection (typically

135    6 to 9 months) for PM mass, elements and filter-based light absorption.  Recently, FT-IR

136    analysis, a non-destructive method, has been performed on IMPROVE samples to reproduce

137 routinely measured compositional data (Debus et al., 2022) and measure the functional group

138 composition of the organic fraction (Ruthenburg et al., 2014, Kamruzzaman et al., 2018).

139 Organic sulfur compounds and organosulfate functional groups were not measured in these

140 studies. FT-IR analysis has also been conducted on other networks and in chamber and field

141 studies to measure organic functional groups (Boris et al., 2021, 2019; Laurent and Allen, 2004;

142 Ruthenburg et al., 2014; Yazdani et al., 2022; Russell et al., 2011). The extracts of nylon filters

143 have been analyzed by ion chromatography (IC) in the IMPROVE network for more than three

144 decades to routinely measure the inorganic ions, sulfate, nitrate, chloride and nitrite.

145 (http://vista.cira.colostate.edu/improve/wp-content/uploads/2020/02/1_Anion-Cation-Analysis-

146 by-Ion-Chromatography-SOP-revision-7.pdf). Although not routinely measured in IMPROVE

147 samples, HMS has been identified in IMPROVE samples using IC (Moch et al., 2020).

148 Organosulfates and MSA have been previously identified in extracts of IMPROVE samples

149 (Chen et al., 2021) using hydrophilic interaction liquid chromatography interfaced to

150 electrospray ionization high-resolution quadrupole time-of-flight mass spectrometry (HILIC-

151 ESI-HR-QTOFMS).

152 The goal of this paper is to assess the stability of four organic sulfur and sulfate

153 containing compounds on polytetrafluoroethylene (PTFE) filters and the suitability of Fourier-

154 transform infrared (FT-IR) spectroscopy to measure these compounds in the IMPROVE network.

155 Measuring organic sulfur compounds on a continuous basis across the US would provide a rich

156 data set to evaluate their sources, concentration, seasonality and trends over time. Four organic

157 sulfur compounds, two organosulfur compounds, methanesulfonic acid,

158 hydroxymethanesulfonate, and two organosulfates, methyl sulfate and 2-methyltetrol sulfate, are

159 evaluated. For these compounds to be measurable in IMPROVE by FT-IR, there must be

160  minimal losses or other changes to the compound during the latency period between collection

161  and analysis (3 – 12 months), and there must be minimal interferences in the spectra.  To achieve

162  this goal, each compound was dissolved in solution, aerosolized and collected on PTFE filters.

163  Collected samples were weighed and analyzed by FT-IR every few days for two months or more.

164  Characterization of the FT-IR spectra as well as changes (or lack therefore of) in the mass

165  loading and spectra over time indicate the potential for the compounds to be measured by FT-IR

166  in IMPROVE samples.  Filter samples, extracted for IC analysis at different time points, indicate

167  stability or chemical changes in the compound on the filter, assists with interpreting gravimetric

168  mass and FT-IR spectra changes.

169  **2 Methods**

170  Two organic sulfur (C-S) compounds, MSA and HMS, and two organosulfates (C-O-S), MS and

171  2-MTS, were selected.  The four compounds were selected for this study based on following

172  three criteria. The compound 1.) has been measured in atmospheric particulate matter and is of

173  interest to the atmospheric science community, 2.) is water soluble so it can be put into solution

174  for atomization, and 3.) is available in high purity form to minimize uncertainty in mass

175  measurement.  Filter samples of the organic sulfur compounds were prepared for FT-IR,

176  gravimetry, IC and ICP-OES analyses by aerosolizing each compound individually and

177  collecting it on PTFE filters (Pall Corporation, 25 mm diameter).  One set of filters was

178  generated for analysis by gravimetry and FT-IR at UC Davis and another set (or sets depending

179  on what was being evaluated) of filters were generated for analysis by IC and ICP-OES at

180  Research Triangle Institute (RTI) following gravimetric analysis at UC Davis.   Analyses of

181  these laboratory filter samples were performed to characterize the compound within infrared

182  spectra and to determine the stability of these compounds over time.

**2.1 Preparation of laboratory filter samples**

Three commercially available standards were used for this study: HMS sodium salt (>97%

purity, TCI America), MSA (100% purity, Sigma Aldrich) and MS sodium salt (100 % purity,

Sigma Aldrich). 2-methytetrol sulfate ammonium salt was synthesized following a published

method (Cui et al., 2018). Each compound was collected on PTFE filters by first preparing an

aqueous solution with a concentration of 0.005 M. For HMS, the solution was acidified with

hydrochloric acid (HCl) prior to aerosolization to obtain samples with atmospherically relevant

pH (pH 2), as pH plays a role in the stability of HMS. 2 µL of 1 M HCl was added to HMS

solution to obtain the final volume of 200 mL for aerosolization. Aerosols were generated using

an atomizer (Kamruzzaman et al., 2018; Ruthenburg et al., 2014) and dried with a diffusion

dryer (Model 3074B Filtered Air Supply, TSI Inc., St. Paul, MN) which produces a high

concentration of poly-disperse submicrometer sized particles allowing for short collection times

and adequately representing the expected response from particles of similar size range in the

atmosphere. Dry particles were collected on PTFE filters (Pall Corporation, 25 mm diameter)

using an IMPROVE sampler with varying collection times (40 to 720 s) at a flow rate of 22.4

L/min.

**2.1.1   Gravimetric mass determination**

Filter mass, before and after particle collection, was measured using an ultra-

microbalance (XP2U, Mettler-Toledo, Columbus, OH) with 0.1 µg sensitivity. Ionizing

cartridges (Staticmaster® Model 2U500, Grand Island NY) housed on a flexible stand

(Staticmaster® Model BF2-1000, Grand Island NY) and Haug strip (Mettler Toledo 11140160,

Columbus, OH) were utilized to help eliminate static for more stable, accurate measurements.

Prior to particle collection, the mass of a filter was determined by the average of 5 mass

206    measurements taken on separate days.  Only filters that weighed within measurements precision

207    for 25 mm filters ($\pm$ 6 µg) for the 5 measurements were used.  After particle collection, filters

208    were allowed to achieve equilibrium at room temperature for 24-hrs.  Filters were weighed for

209    three consecutive days in the 1st week, twice per week during 2nd – 4th weeks and once in the

210    weeks thereafter.  Filters were stored at room temperature (21°C – 27 °C) and relative humidity

211    (30% $\pm$ 10%) to mimic the storage conditions for ambient IMPROVE Teflon filters.  The

212    experiment was ended when the weights were stable for a month or more.

213    **2.2 Infrared spectra collection and processing**

214    FT-IR spectra of the filter samples of each compound were collected using a Tensor II FT-IR

215    spectrometer (Bruker Optics, Billerica, MA) with a liquid nitrogen cooled mercury cadmium

216    telluride (MCT) detector over the spectral range of 4 000–400 $cm^{-1}$.  Filters were placed in a

217    house-built sample chamber that is purged of water and $CO_2$ (PureGas) for 4 min before spectra

218    acquisition (Debus et al., 2019).  Transmission mode measurements were made using 512 scans

219    for each filter at 4 $cm^{-1}$ resolution and ratioed to the most recent (less than 1 h) background

220    spectrum to obtain absorbance spectra using OPUS software (Bruker Optics, Billerica,

221    MA)(Debus et al., 2019).

222    To better visualize functional groups in the organosulfur compounds and minimize the impact of

223    the PTFE scattering and absorption on the spectra, several steps were taken.  Spectra were

224    baseline corrected from 1500 $cm^{-1}$ to 500 $cm^{-1}$, using blank correction and smoothing spline

225    fitting (Kuzmiakova et al., 2016)   The spectral region from 4000 $cm^{-1}$ to 1500 $cm^{-1}$ were

226    baselined using an automated version of the Kuzmiakova et al., 2016 smoothing spline process in

227    AirSpec (Reggente et al., 2019). Regions with large PTFE absorption (1300-1100 $cm^{-1}$, 700-600

228    $cm^{-1}$ and 500-420 $cm^{-1}$) were grayed out in spectra plots and are not considered for peak

229    identification. A baseline corrected spectrum of each compound is shown in supplemental

230    material Figure S1.

**2.3 IC and ICP-OES sample analysis**

232    PTFE filters of each organic sulfur and organosulfate sulfur compound were generated and

233    weighed at UC Davis prior to shipping the filters cold overnight to RTI for IC and ICP-OES

234    analysis. On the day the filters arrived at RTI, the filters were extracted in 50 ml of deionized

235    water (18MΩ cm$^{-1}$, Millipore Milli-Q Darmstadt, Germany), sonicated for 30 minutes in an ice

236    bath and placed on a shaker table in a cold room for 8 hours prior to analysis.  The PTFE filter

237    remained in the extraction vial for the duration of these experiments.

238    IC analysis was performed on Dionex Thermo Scientific ICS-3000 and ICS-6000 (Sunnyvale,

239    CA) instruments using suppression and conductivity detection. For MSA, extracts were analyzed

240    using the AS19 analytical and AG19 guard columns (anion hydroxide method) for initial

241    extraction efficiency tests and AS28 analytical and AG28 guard columns (hydroxide method) for

242    the subsequent analyses to evaluate changes over time.  HMS and MS extracts were analyzed

243    with AS12A analytical and AG12A guard columns (anion carbonate method), which has been

244    shown to provide sufficient separation of HMS and sulfate, but not separation of sulfite/bisulfite

245    and HMS (Dovrou et al., 2019).   MS extracts were analyzed with AS12A analytical and AG12A

246    guard columns (anion carbonate method), the same method as HMS. An IC method for analyzing

247    2-MTS had not been developed and evaluated prior to this work.  Eluent concentrations and flow

248    rates were optimized for best separation of all ions of interest.

249    ICP-OES, used to measure total sulfur on the filter, was performed on a Thermo Scientific iCAP

250    7600 duo analyzer (Bremen, Germany). The ICP-OES was run in axial mode using a sprint valve

251    and data were collected at 180.731 nm. The ICP-OES system was calibrated using the sulfate

252 calibration standards and validated using the sulfate calibration verification solutions described

253 below.

254 IC and ICP-OES systems were calibrated with calibration standards prepared via serial dilutions

255 of single source stock standards using a primary source. A secondary source was used to prepare

256 calibration verification solutions to validate the instrument calibration for all compounds except

257 for 2-MTS, for which a second source standard was unavailable.

258 Primary and secondary sources of National Institute of Standards and Technology (NIST)-

259 traceable solutions were purchased and used to prepare calibration standards and calibration

260 verification solutions respectively, for sulfate analyses by both IC and ICP-OES. When NIST-

261 traceable solutions were unavailable, salts were used to prepare calibration standards and

262 calibration verification solutions for MSA, HMS, and MS. Vendor information for primary and

263 secondary sources are provided in Table S2 in supplemental material. Certified American

264 Chemical Society (ACS)-grade sodium carbonate ($Na_2CO_3$) obtained from Fisher Scientific

265 (Fairlawn, NJ) and sodium bicarbonate ($NaHCO_3$) obtained from EMD Sciences (Gibbstown,

266 NJ) were used to prepare IC eluent when using anion carbonate methods for analyses. Potassium

267 hydroxide eluent generator cartridges purchased from Thermo Scientific were used for eluent

268 preparation for analyses conducted with anion hydroxide methods. NIST-traceable, 1000 µg/mL

269 stock solutions of yttrium (Y) and cesium (Cs) obtained from High Purity Standards (Charleston,

270 SC) were used to for internal standard and ionization suppression, respectively for ICP-OES

271 measurements.

272 **3 Results and Discussion**

273 **3.1 Methanesulfonic acid**

274 **3.1.1 Gravimetry**

275 Mass changes, measured by gravimetry, for four methanesulfonic acid filter samples with masses

276 ranging from 64 µg to 80 µg are shown in Figure 1. Mass decreases steadily during the first

277 month to approximately 50% of the initial mass. During the second month of measurements, the

278 mass remains constant (50 ± 6%).
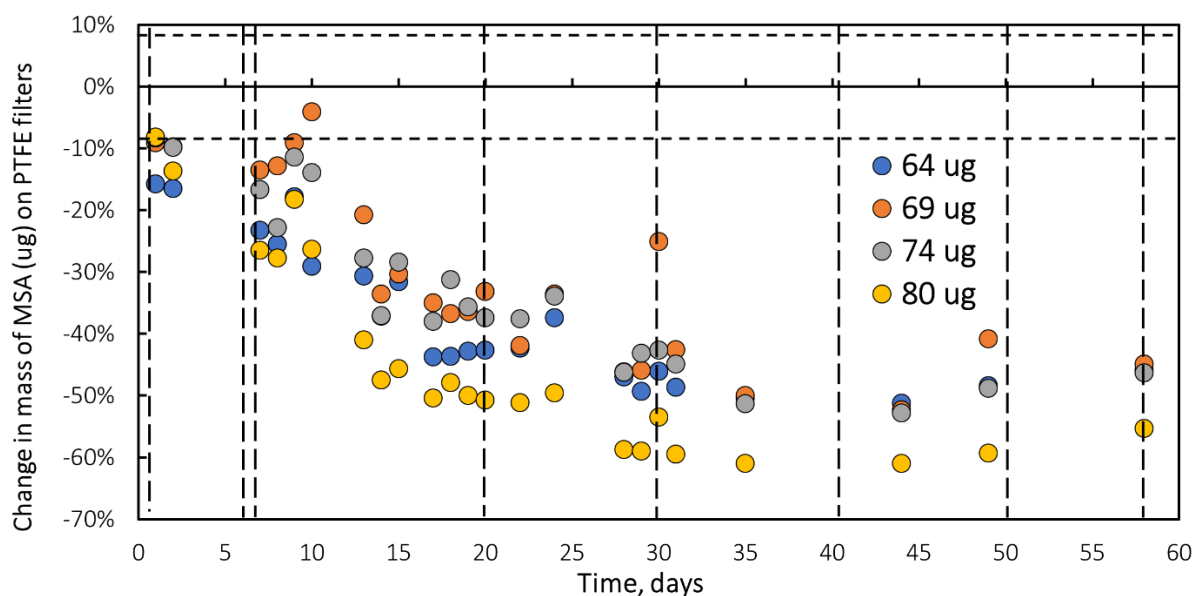
279

280 **Figure 1. Change in mass of methanesulfonic acid (MSA) collected on PTFE filters over a**

281 **2- month period under laboratory conditions (24 ˚C). Dotted vertical lines indicate FT-IR**

282 **analysis. Horizontal broken line indicates mass balance precision. Colors indicate initial**

283 **masses of samples.**

284 **3.2 FT-IR**

285 Methanesulfonic acid ($CH_3SO_3H$) is composed of a methyl group attached to a sulfonic acid

286 [$S(=O)_2$—OH], via a C-S bond. Methanesulfonic acid aerosols collected on PTFE filters have

287   peaks associated with $CH_3$, $SO_3$, S-OH and C-S bonds (Figure 2).  Observed peaks (Figure 2)

288   can be ascribed to portions of the molecule based on previous FT-IR and Raman work (Lee et

289   al., 2019; Zhong and Parker, 2022; Chackalackal and Stafford, 1966).  The peaks at 1342 $cm^{-1}$

290   and 536 $cm^{-1}$ arise from S=O bonds in MSA and are shifted compared to inorganic peaks at 1130

291   $cm^{-1}$, 620 $cm^{-1}$ (Larkin, 2018) or organic sulfate $SO_4$ peaks at ~1380 $cm^{-1}$ (Larkin, 2018; Lin-

292   Vien et al., 1991). The peak at 895 $cm^{-1}$ is attributable to S—OH  (Zhong and Parker, 2022) and

293   the peak at 766 $cm^{-1}$ is attributable to C-S (Lee et al., 2019). C-H peaks are observed at 3039 $cm^{-}$

294   $^1$, 2951 $cm^{-1}$, 1414 $cm^{-1}$ and 987 $cm^{-1}$ (Chackalackal and Stafford, 1966).  The broad peak at 3248

295   $cm^{-1}$ is suggested to be water as (Zeng et al., 2014) showed that this peak in MSA infrared

296   spectra increases with increasing RH.  These peaks, particularly strong peaks, were similar to

297   spectral absorbance of MSA from reference spectra (Spectral Database for Organic

298   Compounds,SDBS, 2022), and Table S1 in Supplemental Materials compares the observed and

299   reference peaks.
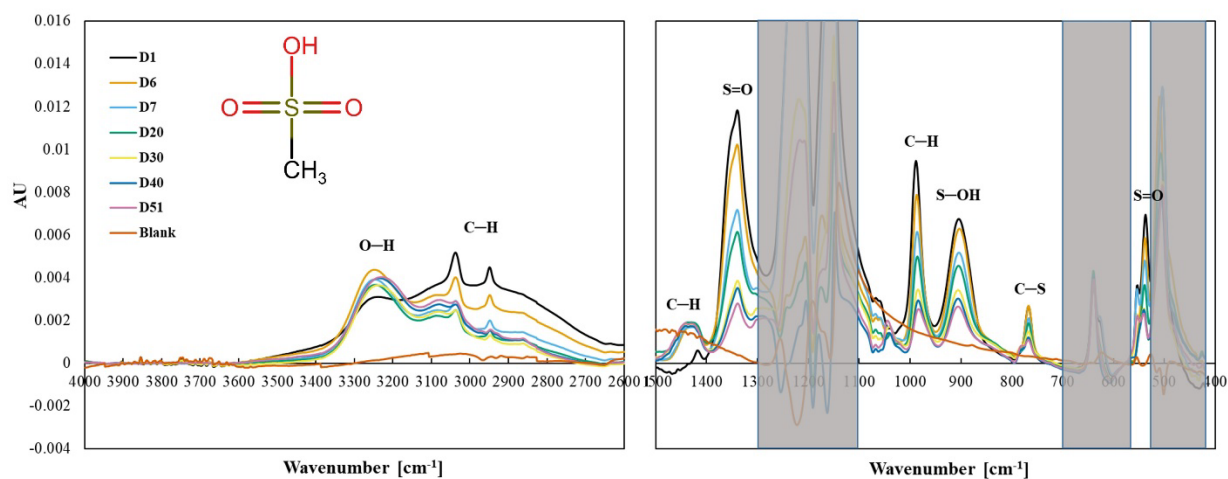
300

301   **Figure 2. Changes in the spectra of MSA over a 2- month period, denoted by number of**

302   **elapsed days. The shaded area indicates the absorbance regions of PTFE filter.**

303    The MSA infrared peaks of $SO_3$ (1342 cm$^{-1}$), C—H (987 cm$^{-1}$), S—OH (895 cm$^{-1}$), C-S (766 cm$^{-}$

304    $^1$), and S=O (536 cm$^{-1}$) decrease rapidly in the first 30 days, consistent with the decline in mass

305    during that time.  The spectra suggest that MSA is volatilizing off the filter, even though this is

306    inconsistent with the low vapor pressure of MSA (Knovel - Yaws' Critical Property Data for

307    Chemical Engineers and Chemists - Table 12. Vapor Pressure - Organic Compounds, log P = A -

308    B/(T + C), 2022), 0.00022 mmHg at 20°C).  The three spectra obtained on days 30, 41 and 51

309    show only small decreases which is mostly consistent with the lack of mass changes during those

310    days.

311    Not all peaks show consistent loss during the first month and little change during the second

312    month. The C-H peaks at 3039 cm$^{-1}$ and 2942 cm$^{-1}$ behave slightly differently, reaching stability

313    (with some minor random variability) earlier (day 20) than most other peaks. The weak peak at

314    1414 cm$^{-1}$ (ascribed to $CH_3$) increased and broadened to 1445 cm$^{-1}$ - 1400 cm$^{-1}$ after the initial

315    spectra was collected and remained fairly stable for the duration of the experiment. The peak at

316    3250 cm$^{-1}$, increased rapidly followed by fluctuations, and then varies somewhat but remained

317    fairly consistent for the duration of the experiment, not unlike the behavior of the 1414 cm$^{-1}$

318    peak.  One possible cause for these spectra changes in the spectra is water vapor condensing on

319    the particles after collection. MSA is hygroscopic and although it effloresces at about RH = 50%,

320    (Peng and Chan, 2001; Tang, 2020; Zeng et al., 2014), Zeng et al., 2014 shows that there is some

321    water associated with the particles below 50% RH, which is consistent with the FT-IR spectra

322    (Figure 3), particularly the 3248 cm$^{-1}$ peak.  If water is indeed the cause, the change in the 3248

323    cm$^{-1}$ peak can be explained by a very low RH in the particle generation and collection system

324    (lower initial peak) and a higher RH (RH = 30 $\pm$ 10%) in the lab (increase in peak).  The change

325   in the 1414 cm$^{-1}$ peak above 1400 cm$^{-1}$ behaves similarly and can be associated with OH

326   suggesting uptake of water after the initial FT-IR spectra was collected.

327   Another possibility is that ammonia is absorbing onto the MSA. Ammonium absorbs in both the

328   3250 cm$^{-1}$ and 1500-1400 cm$^{-1}$ regions (Boer et al., 2007; Zawadowicz et al., 2015) and when

329   comparing  MSA spectra to ammonium sulfate spectra, they show very similar peak absorbance

330   and shapes in these two regions suggesting. This suggests that the cause of these peaks is

331   ammonium (Supplemental Material, Figure S2).

332   A third possible cause for these changes is that MSA may be fragmenting into formaldehyde

333   ($CH_2O$), that partitions into the gas phase, and sulfite ($SO_3$) (Kwong et al., 2018a).  However,

334   this would show a decrease in CHC-H peaks and a shift in the SOS=O peaks, neither of which

335   are observed in the spectra.  The rapid decrease in peak height during the first month and then

336   little decrease or no trend during the second month, suggests that MSA is volatilizing off the

337   filter initially, but then has a slow decline, offset by increases in water or ammonium.

338   **3.1.3 IC and ICP-OES**

339   Twenty PTFE filters with MSA (14 µg – 32 µg; 60 µg – 144 µg) were shipped to RTI for

340   extraction and analysis by IC and ICP-OES. Each extract was analyzed by both IC and ICP-OES.

341   Recoveries of MSA from PTFE filters was $55 \pm 5\%$ for IC and $51 \pm 5\%$ for ICP-OES.

342   Calibration verification solution recoveries were $96 \pm 5\%$ for IC and $101 \pm 3\%$ for ICP-OES

343   analyses, suggesting that the lower recoveries from the PTFE filter are due to incomplete

344   extraction and/or losses occurring during shipment. To evaluate losses during shipping, six

345   samples were collected, weighed, and analyzed by FT-IR, shipped to RTI and then sent back to

346   UC Davis and analyzed with gravimetric and FT-IR analysis 9 days after initial measurements.

347   The mass loss ($19 \pm 7\%$) during this period was similar to mass loss for filters that remained in

348 the UC Davis laboratory for ~8 days ($22 \pm 6\%$). Spectral changes in shipped filters were similar

349 to changes in spectra that occurred during the first week for filters that remained at UC Davis.

350 To evaluate changes in mass and composition on PTFE filters over time, 6 filters ($42 \, \mu g$ – $63 \, \mu g$)

351 were shipped to RTI and extracted on days 0, 30, and 61. These filters had consistent recoveries

352 over time of $57 \pm 6\%$ for IC and $55 \pm 6\%$ for ICP-OES.  The IC results indicate that MSA did

353 not change chemically during this time period, supporting the FT-IR spectral results.  The mass

354 and spectral data indicate that the lower extraction efficiency was not due to loss of MSA off the

355 filter during shipping and suggest that the limitation is extraction efficiency. Despite low

356 extraction efficiencies and difference in behavior over time from FT-IR measurement, the FT-IR,

357 gravimetry and IC results suggest that a lower-bound of MSA can be measured on PTFE filters

358 in IMPROVE by FT-IR.

359 **3.2 Hydroxymethanesulfonate**

360 **3.2.1 Gravimetry**

361 Mass changes in three hydroxymethanesulfonate sodium salt ($HOCH_2SO_3Na$) filter samples with

362 mass loadings of ~62 $\mu g$ per filter are shown (Figure 3). Mass decreases steadily for 1.3 months

363 to a maximum loss of 38% and then remains constant ($38 \pm 3\%$) for the rest of the experiment

364 (4.1 months).  Similar results were obtained for filters weighing approximately 30 $\mu g$/filter of

365 HMS.

366

367
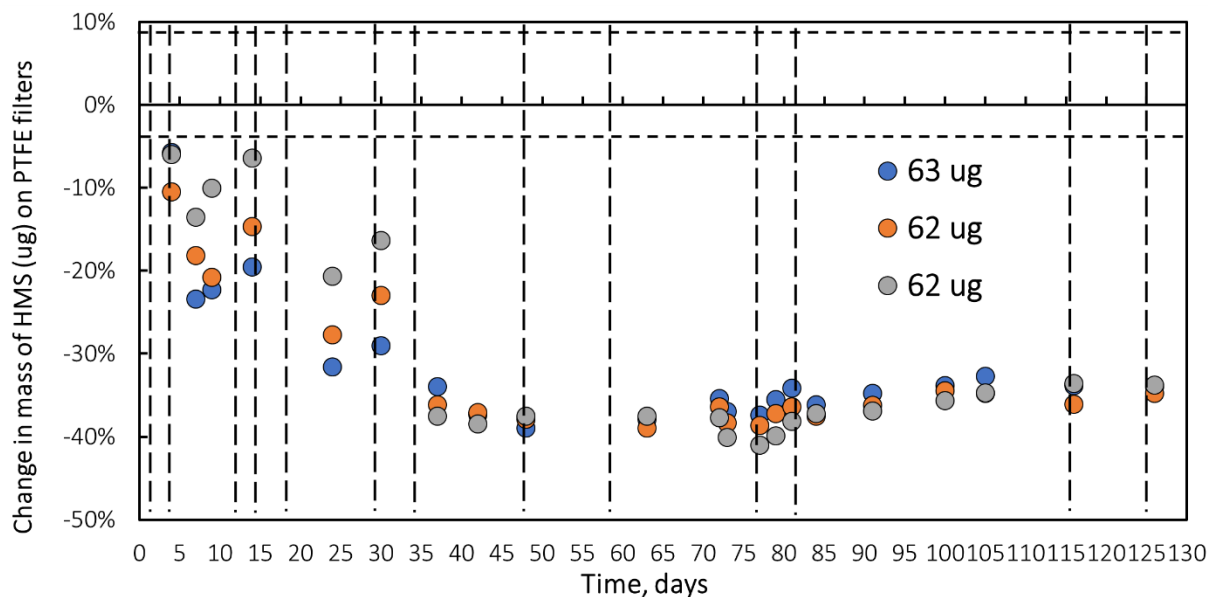
**Figure 3. Mass behavior of hydroxymethanesulfonate (HMS) over 125 days under laboratory conditions (~24°C). Dotted vertical lines indicate FT-IR analysis. Horizontal broken line indicates mass balance precision.**

**3.2.2 FT-IR**

HMS (HOCH$_2$SO$_3$H) is a sulfonic acid compound with C-S bond, where the S bond is part of a sulfonic acid group [S(=O)$_2$─OH], and the carbon is attached to an –OH functional group, similar to MSA except with the OH functional group attached to the carbon. The chemical used in our study has a sodium cation on the sulfonic acid group. HMS aerosol collected on PTFE filters have three infrared peaks (1094 cm$^{-1}$, 1041 cm$^-$and$^1$, 611 cm$^{-1}$) between 1500 and 500 cm$^{-1}$, although the peak at 611 cm$^{-1}$ is obscured by PTFE absorption, and O-H and C-H peaks between 4000 cm$^{-1}$ and 1500 cm$^{-1}$ (Figure 4).

379
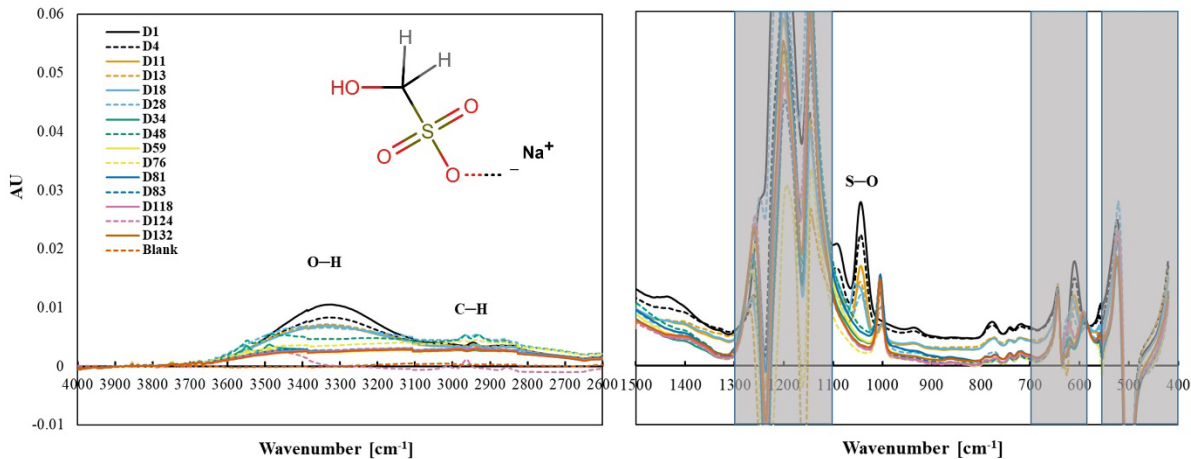
**Figure 4. Changes on the functional group frequency region of hydroxymethanesulfonate**

**(HMS) over 4.1 months.**

Observed peaks at 1094 cm$^{-1}$ and 1041 cm$^{-1}$ are similar to the 1080 cm$^{-1}$ and 1040 cm$^{-1}$ peaks

identified as S-O or S=O bonds in FT-IR spectra of Na HMS (Sato et al., 1984) and of HMS

(Larkin, 2018; Shurvell, 2006). A weak band at 611 cm$^{-1}$ is like due to C-S (Lin-Vien et al.,

1991; Sato et al., 1984) or S-O (Sato et al., 1984) but is obscured by PTFE absorbance. Above

1500 cm$^{-1}$ and similar to many aliphatic organic molecules, an O–H (broad peak centered near

3300 cm$^{-1}$) and C-H (below 3000 cm$^{-1}$) peaks were observed (Pavia et al., 2008; Shurvell, 2006).

Observed peaks are similar to spectral absorbance, although not all peaks in the reference spectra

(AIST: SDBS, 2022, See Table S1 in Supplemental Material) are observed in the measured

spectra. HMS has a very low vapor pressure (0.00000073 mmHg), (U.S. EPA. Comptox

Chemicals Dashboard, 2022) indicating that HMS should not volatilize off the filter.

All peaks below 1500 cm$^{-1}$ decrease and are no longer visible by day 34, consistent with

the decline but not the extent of decline in mass as the HMS peaks are completely gone and the

mass has only decreased by 40%. This behavior is most clearly observed in the peak at 1041 cm$^{-1}$, but also observed in 1094 cm$^{-1}$ peak (Figure 4). Similar to the S-O/S=O peaks, C-H peaks

397   decline during the first 34 days and then completely disappear. The O-H peak, centered around

398   3300 cm$^{-1}$, disappears more slowly, but like the S-O and C-H peaks, is gone by the end of the

399   experiment. Counter balancing the loss of mass, a new peak becomes visible at 1003 cm$^{-1}$ after

400   11 days and increases for the rest of the study. The peak at 1003 cm$^{-1}$ is tentatively identified as

401   bisulfate (Boer et al., 2007; Krost and McClenny, 1994).  The small peak centered around 3450

402   cm$^{-1}$ becomes evident as the O-H peak disappears and may indicate the presence of condensed

403   water (Boer et al., 2007).

### 3.2.3 IC and ICP-OES

405   Sixteen HMS PTFE filters were analyzed by IC with recoveries of $65 \pm 4\%$ and calibration

406   verification solution recoveries of $94 \pm 5\%$.  ICP-OES analysis was not performed on these

407   filters.  Eight additional HMS filters (65 µg – 100 µg) were shipped to RTI and 2 filters were

408   extracted and analyzed by IC and ICP-OES on each of the following days 0, 30, 61, and 101.

409   The sulfur mass losses in IC (Figure S3, Supplemental Material) over the 101 days is ~60% loss

410   from the initial weighed mass or about 39% loss assuming a constant extraction efficiency of

411   65% for all samples and is in agreement with the 38% decrease in mass on the filter measured by

412   gravimetry. Similar results were obtained for ICP-OES.  IC analysis (Figure 5) confirms the

413   samples are mostly HMS on day zero but over time the HMS is converted to sulfate (sulfate and

414   bisulfate are indistinguishable in IC), supporting assignment of the 1003 cm$^{-1}$ infrared peak to

415   inorganic bisulfate.  A small amount of the HMS may be converting to sulfate in solution or the

416   column, but the measured changes are much larger than what is expected due to that mechanism

417   alone.  The small amount of HMS that is measured by IC on day 60 and 101 are near detection

418   limits for IC which corroborate the absence of HMS in the FT-IR spectra after two months. The

419   IC and FT-IR results both show a conversion of HMS into sulfate indicating that HMS is not

420    stable and cannot be quantified reliably on PTFE filters in IMPROVE by either FT-IR or IC. In

421    Moch et al. (2020), HMS did not degrade over time under cold storage conditions on nylon

422    filters from IMPROVE suggesting that storage or perhaps filter type may play an important role

423    in HMS degradation on filters.
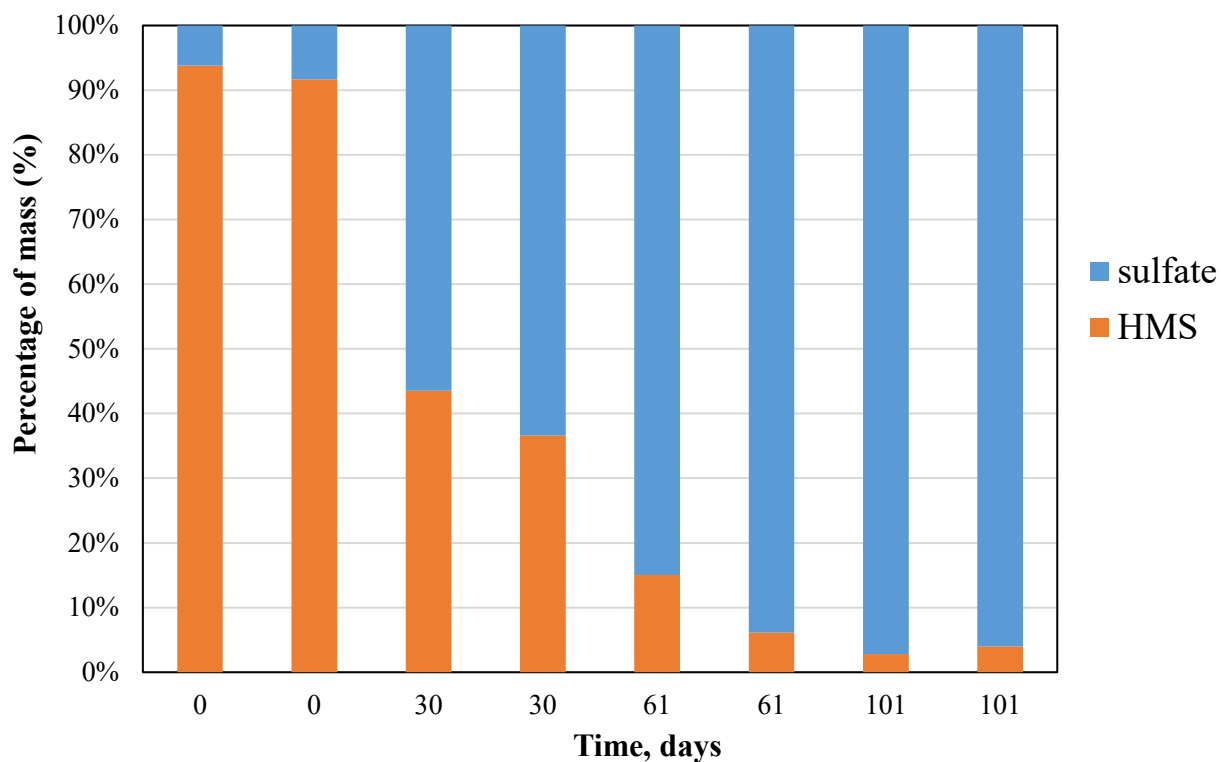
424

425    **Figure 5. Percentage of HMS and sulfate measured by IC. Eight PTFE filters were**

426    **extracted and analyzed in pairs over 101 days.**

427    **3.3 Methyl sulfate**

428    **3.3.1 Gravimetry**

429    Mass measurements of methyl sulfate salt over a 4 -month period were within measurement

430    uncertainty for the three filters loaded with approximately 30 µg of methyl sulfate (the change

431    over time was indistinguishable from zero). For the 60 µg filters (Figure 6), the first 2 months

432  and the last two weeks mass change were within measurement uncertainty ($\pm$ 6 µg). However,

433  for about a month, between day 70 and 100, much of the data (except day 91) is outside of

434  measurement uncertainty, indicating mass loss of between 10 and 20%. During this period only

435  one spectrum (day 79) was collected, and it does not support mass loss. Day 100 spectra, and all

436  spectra collected through the end of the study, for all three 60 ug loadings, filter samples

437  confirms no changes in the MS compound. Mass and spectral data indicate stability of mostly

438  stable MS on filters under ambient laboratory condition (24°C).
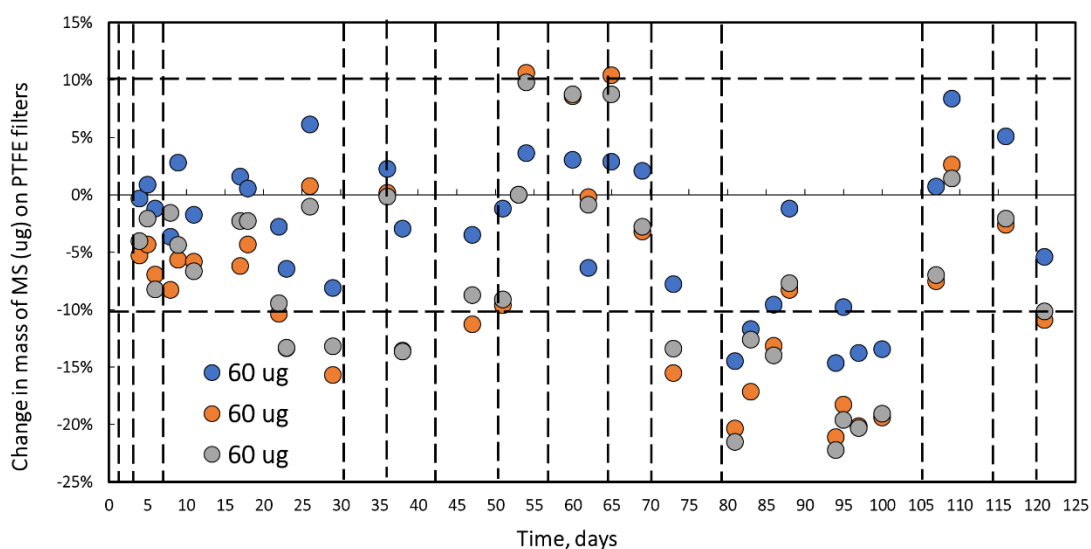
439

440  **Figure 6. Mass behavior of methyl sulfate (MS) standard over 4 months. Dotted vertical**

441  **lines indicate FT-IR analysis. Horizontal broken line indicates mass balance precision for**

442  **PTFE 25- mm diameter filters.**

443  **3.3.2 FT-IR**

444  Methyl sulfate ($CH_3SO_4H$) is composed of a methyl ($CH_3$) group attached to a sulfate ($SO_4$)

445  group with C-O-S bond.  The chemical used in this study is sodium methyl sulfate ($CH_3SO_4Na$).

446  Methyl sulfate aerosol collected on  PTFE filters has two peaks between 4000 cm$^{-1}$ and 2000 cm$^{-}$

447  $^1$ and eight peaks between 1500 and 500 cm$^{-1}$ (Figure 7), similar to reference spectra in Table S1

448 (Spectral Database for Organic Compounds,SDBS, 2022). The doublets observed at 1020 cm$^{-1}$,

449 1000 cm$^{-1}$ and the nearly overlapping peaks at 795 cm$^{-1}$ and 784 cm$^{-1}$ are identified as S-O-C by

450 both FT-IR  (Chihara, 1958; Lloyd et al., 1961; Lloyd and Dodgson, 1961; Segneanu et al., 2012;

451 Shurvell, 2006) and Raman (Okabayashi et al., 1974). The S─O peaks from sulfate are observed

452 around 1073 cm$^{-1}$ and 591 cm$^{-1}$ in the spectra, similar to the previous study where peaks from

453 591 cm$^{-1}$ to 593 cm$^{-1}$,  and at 1063 cm$^{-1}$ (solid) and 1081 cm$^{-1}$ (solution) were ascribed to sulfate

454 in potassium methyl sulfate (Chihara, 1958). There is a weak S=O peak at 1458 cm$^{-1}$ (Segneanu

455 et al., 2012).  The O-H group (assuming the Na ion was replaced by H for some of the

456 molecules) at 3500 cm$^{-1}$ is also fairly weak. All collected spectra for one sample are shown, with

457 the exception of day 91 data, which appeared to be anomalous (Supplemental Material, Figure

458 S4 all spectra including day 91).

459 The stability of the spectra over 4 months suggests that MS is stable when collected on a PTFE

460 filter. There were no major or consistent changes in peaks associated with S─O─C, S─O, Na-O

461 and C─H.

462 The pattern of change in the peak height of the 3500 cm$^{-1}$ peak does not correlate with the

463 change in mass. Day 1 and day 30 spectra have smaller O-H peak intensities prior to mass

464 decline, compared to and the O-H peak in the spectrum from day 79, when mass had decreased

465 the mass is low, is higher than both.  No consistent difference in the FT-IR spectra was observed

466 on day 79 (low gravimetric mass day) or the following days (days 105 – 120) suggesting that the

467 mass loss seen in the gravimetric data is erroneous.  The high melting and boiling points of MS

468 are 96 °C and 298 °C, respectively and the low vapor pressure of 0.0038 mmHg (U.S. EPA.

469 Comptox Chemicals Dashboard, 2022) indicating that MS is not volatilizing off the filter.
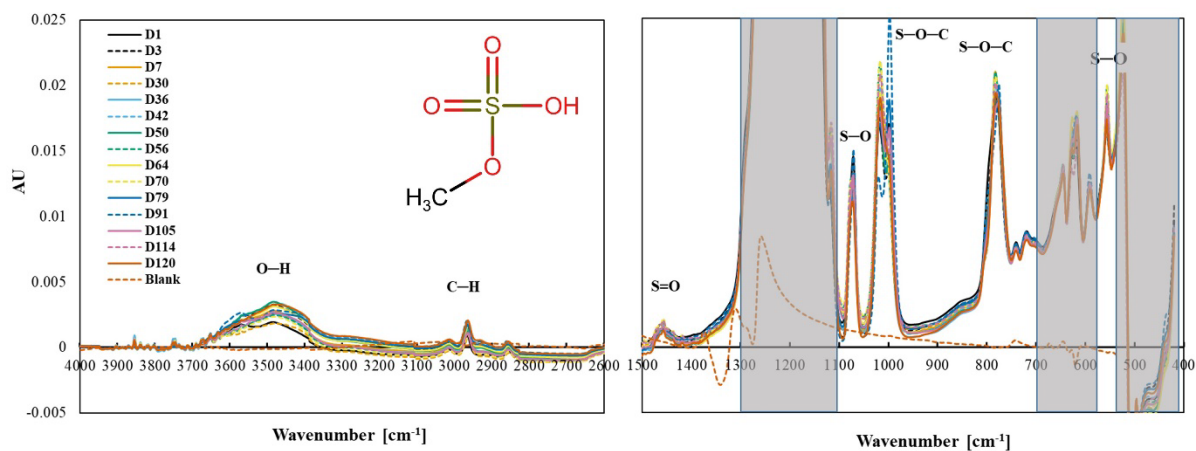
**Figure 7. Changes in the spectra of MS over a 4- month period. The shaded area indicates the absorbance regions of PTFE filter.**

### 3.3.3 IC and ICP-OES

Sixteen PTFE samples, eight with mass loadings between 38 µg – 57 µg and eight with higher mass loadings, between 98 µg – 118 µg, were prepared for IC and ICP-OES analysis.  Eight PTFE filters were extracted on day 0 and recoveries were $60 \pm 1\%$ for IC and $87 \pm 3\%$ for ICP-OES analyses. Recoveries of calibration verification solutions were $100 \pm 1\%$ for IC and $97 \pm 6\%$ for ICP-OES.  Additional filters were extracted on day 39 and 61 showed recoveries consistent with recoveries measured during the initial extracts, $59 \pm 2\%$ for IC and $86 \pm 4\%$ for ICP-OES.  The overall lower mass recovery is indicative that not all MS is extracted from the filter and the lower recoveries by IC compared to ICP-OES, suggests that MS is converting to another sulfur compound in solution.  The consistency in recoveries over time indicates stability of MS on PTFE over this time period, which is in agreement with the mass stability of as shown by gravimetric over the course of the experiment. Unfortunately, filters were not extracted during the time period when the gravimetric results show a small deviation from stability.

487    MS is stable on a PTFE filter as indicated by gravimetry, FT-IR and IC suggesting that at least

488    some atmospherically relevant organosulfates can be measured on PTFE filters in IMPROVE by

489    FT-IR.

490    **3.4 2-Methyltetrol sulfate**

491    **3.4.1 Gravimetry**

492    Mass changes in three 2-methyltetrol sulfate ($C_5H_{11}SO_7$) filter samples with concentrations from

493    55 µg to 57 µg are shown in Figure 8. Mass decreases during the first 23 days to 73% of the

494    initial mass (25% ± 2%).  No additional mass loss was observed after 25 days. Mass behavior

495    indicates a loss of 2-MTS on filters under ambient laboratory condition (24°C).  Similar results

496    were obtained for filters weighing approximately 40 µg.
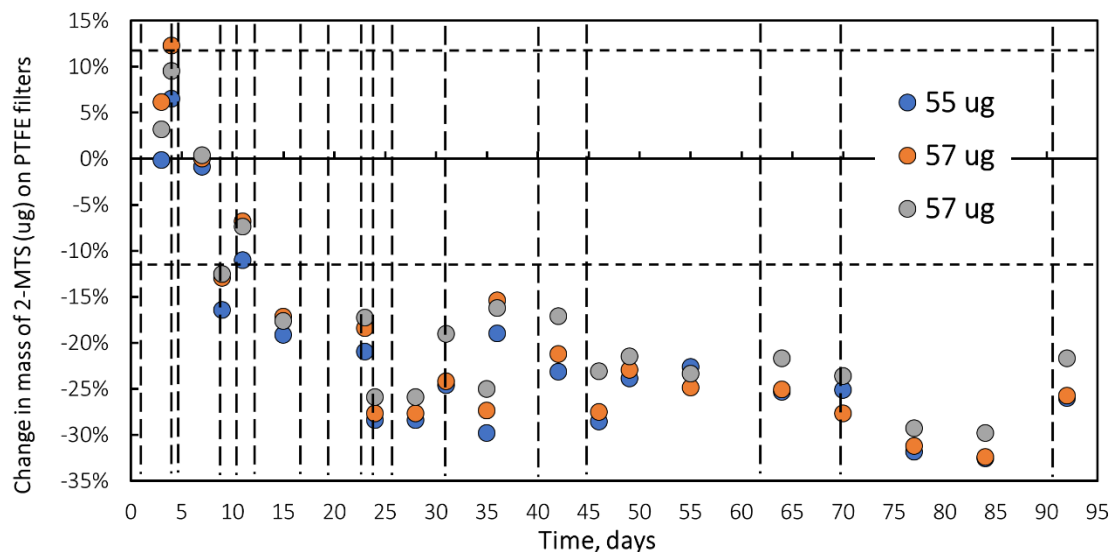
497

498    **Figure 8. Change in mass of 2-MTS collected on PTFE filters over a 3-month period under**

499    **laboratory conditions. Dotted vertical lines indicate FT-IR analysis. Horizontal broken red**

500    **line indicates mass balance precision.**

### 3.4.2 FT-IR

2-Methyltetrol sulfate ($C_5H_{11}SO_7$) is a branched compound with 3 units of –OH, one methyl

group and a sulfate group. Like methyl sulfate, 2-methyltetrol sulfate is an organosulfate and has

a C-O-S bond.  2-MTS collected on PTFE filters has broad, organic-related peaks between 4000

$cm^{-1}$ and 2500 $cm^{-1}$ and four peaks between 1500 and 500 $cm^{-1}$ (Figure 9). Observed peaks can

be ascribed to functional groups with the molecule based on previous FT-IR and Raman work

(Lloyd et al., 1961; Lloyd and Dodgson, 1961; Bondy et al., 2018; Fankhauser et al., 2022).
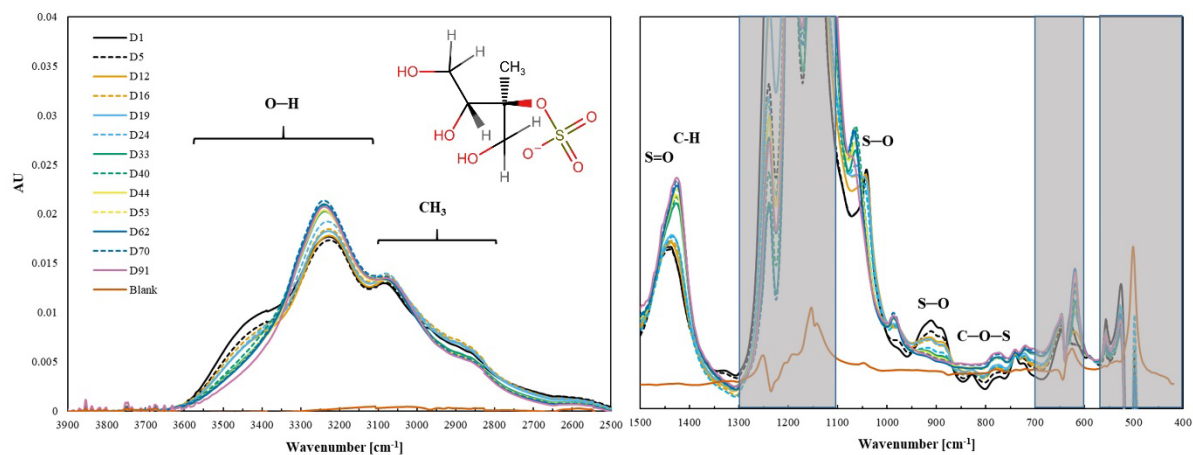
**Figure 9. Changes in the spectra of 2-MTS over a 3-month period. The shaded area**

**indicates the absorbance regions of PTFE filter.**

The observed peak at 1041 $cm^{-1}$ is ascribed to S-O stretch (Bondy et al., 2018; Fankhauser et al.,

2022), as it is similar to the peak of MS at 1050 $cm^{-1}$ (Lloyd et al., 1961; Lloyd and Dodgson,

1961).  The doublet at 908 $cm^{-1}$ and 898 $cm^{-1}$ correspond to symmetric and asymmetric stretch of

S-O of 2-MTS (Fankhauser et al., 2022). The weak peak at 827 $cm^{-1}$ is tentatively assigned to C-

O-S stretch based on Raman spectra of 3-MTS (Bondy et al., 2018). The peak at 1446 $cm^{-1}$ is

tentatively assigned  to asymmetric S=O stretch based on density functional theory of FT-IR

spectra of 2-MTS (Fankhauser et al., 2022) and the assignment of S=O to peak at 1448 $cm^{-1}$ in

methyl sulfate (Bondy et al., 2018).  However, this peak was suggested to be due to C-H using

519  density functional theory of Raman spectra of 2-methyltetrol sulfates (Bondy et al., 2018) and

520  commonly ascribed to $CH_2$ in organic molecules at ~1465 cm$^{-1}$ (Pavia et al., 2008).  We decided

521  to assign this to S=O because the sulfate related peaks are strong and the C-H peaks are very

522  weak in this molecule. In the higher frequency region, the very subtle peak at 2879 cm$^{-1}$ is

523  ascribed to C-H stretch and the large broad peaks at 3065 and cm$^{-1}$, 3210 cm$^{-1}$ and shoulder at

524  3426 cm$^{-1}$ may be attributable to –OH stretch (Larkin, 2018; Shurvell, 2006; Bondy et al., 2018;

525  Fankhauser et al., 2022) or inorganic –NH stretch (Boer et al., 2007; Larkin, 2018). Our tentative

526  peaks assignments of ammonium at 3210 cm$^{-1}$ and 3065 cm$^{-1}$ and OH at 3426 cm$^{-1}$ are based on

527  changes in spectra discussed below.

528      Most of 2-MTS infrared peaks decreased and disappeared over time, consistent with the

529  decline in mass.  The S-O peaks at 1041 cm$^{-1}$, 908 cm$^{-1}$ and 898 cm$^{-1}$ decreased and were gone

530  by day 40. The weak C-O-S peak at 827 cm$^{-1}$ disappeared by day 26. The C-H region at 3000-

531  2800 cm$^{-1}$ decreased, similar to the changes in S-O-C peaks. However, some peaks shifted or

532  new peaks formed.  New peaks (or possibly shifts from 1041 cm$^{-1}$ and 908 cm$^{-1}$ doublet) at 1066

533  cm$^{-1}$ and at 987 cm$^{-1}$ appear on day 40 and then increase slightly over time. The S=O peak at

534  1446 cm$^{-1}$ behaves differently from other 2-MTS peaks and increases slightly until day 33 when

535  the peak height increased significantly and shifted to 1420 cm$^{-1}$ where it continues to grow

536  increase over time. Two peaks at 3210 cm$^{-1}$ and 3065 cm$^{-1}$ increased whereas the region around

537  3450-3550 cm$^{-1}$ decreased, indicating that the shoulder at 3450 cm$^{-1}$ arises from a different bond

538  than the peaks at 3210 cm$^{-1}$ and 3065 cm$^{-1}$.

539  The changes in the spectra indicate a change in the chemical composition on the filter.  2-MTS is

540  no longer present by mid-way through the experiment as evidenced by the disappearance of S-O,

541  C-O-S, C-H and O-H peaks.  This result is supported by a study of ambient 2-MTS that showed

542     that the atmospheric lifetime of 2-MTS is to be about 16 days (Chen et al., 2020). Intermediate

543     oxidation products of 2-MTS transformation include other organosulfates such as 2-

544     methylglyceric acid organosulfate ($C_4H_7SO_7$, MGOS) and glycolic acid organosulfate ($C_2H_3SO_6$,

545     GAS) (Zhao et al., 2020; Wei et al., 2020) and the final product is likely inorganic $(NH_4)_2SO_4$

546     (Harrill, 2020; Zhao et al., 2020).  Raman spectra of MGOS (Bondy et al., 2018) indicate that the

547     spectra at the end of the experiment could be 2-MGOS.  The increased peak at 3210 $cm^{-1}$ and

548     3065 $cm^{-1}$ could be associated with –OH stretch and $CH_3$ asymmetric stretch of 2-MGOS and the

549     1420 $cm^{-1}$ (C-H), 1066 $cm^{-1}$ (S-O) and 987 $cm^{-1}$ ($SO_4^{2-}$) match the final spectra well.  The

550     carbonyl group in 2-MGOS is very weak in the Raman spectra and indistinguishable from a

551     blank filter in the final FT-IR spectra in this project.  Alternatively, the final spectra could be

552     ammonium sulfate as indicated by peaks at 3210 $cm^{-1}$, 3065 $cm^{-1}$  and 1420 $cm^{-1}$  which are

553     indicative of ammonium, however, the 1066 $cm^{-1}$ and 987 $cm^{-1}$ peaks are lower than typically

554     observed for inorganic ammonium sulfate (Boer et al., 2007; Zawadowicz et al., 2015)

555     suggesting this is not inorganic sulfate. There are limited FT-IR or Raman spectra of the many

556     oxidation products of 2-MTS so definitive identification is not possible and it is likely that there

557     is a mixture of oxidation products present on the filter.

558     To further evaluate the possible compounds on the filter at the end of the experiment, mass loss

559     calculations were performed using the molecular weight of 2-MTS and each product (MGOS,

560     GAS and ammonium sulfate).  If 2-MTS is converted completely to MGOS, the mass loss would

561     be only 7%.  If 2-MTS is converted completely to GAS, the mass loss would be 28% and if 2-

562     MTS is converted completely to ammonium sulfate the mass loss would be 39%.  These values

563     span the observed mass loss at 25% which suggesting that the compounds on the filter are of an

564     intermediate type and still in the organosulfate form not inorganic ammonium sulfate.

### 3.4.3 IC and ICP-OES

Sixteen PTFE samples, eight with mass loading between 11– 28 µg and eight with higher mass loadings, between 37 – 46 µg were extracted immediately upon receipt at RTI. The IC showed low sensitivity to 2-MTS detection and results are not reported so no additional information was available about what compounds the 2-MTS may have change into.  Given that ICP-OES measures sulfur and not individual compounds, the results from this method do not provide insight into chemical conversions on the filter but are briefly discussed in the supplemental material (Figure S5).

### 4 Conclusions

The stability and therefore potential for FT-IR to measure organosulfur and organosulfates collected on PTFE filters varies by compound. MS has the highest potential to be measured on PTFE filters in IMPROVE samples by FT-IR, due to its minimal mass change and no spectral changes. Consistent recoveries by IC and ICP-OES over multiple months of analysis support the conclusion that MS is stable on the filters.  Consistent results from analysis at UC Davis and RTI suggest robustness to storage, shipping and handling conditions.  MS is one of many organosulfates observed in the atmosphere and not necessarily representative of organosulates in general as indicated by 2-MTS.  Gravimetric mass suggests some (30%) mass loss from 2-MTS samples on the PTFE filter, over a three-month period. FT-IR suggests that 2-MTS is unstable on PTFE filter and changing into different compound(s), likely still an organosulfate.  FT-IR and gravimetry show that MSA can be measured from PTFE filters but due to volatility off the filters a lower bound of MSA is measured (i.e., less than the amount of MSA in the atmosphere). IC further confirmed that MSA did not chemically change while on the filter.  Infrared peaks in HMS spectra mid-way through the experiment indicate that HMS is not

588   stable on PTFE filters and likely converts to bisulfate. IC indicates that HMS is changing to

589   (bi)sulfate over time.  Further investigations of measurements by FT-IR on PTFE of other

590   organosulfates are warranted to evaluate the extent to which the organosulfate functional group

591   can be quantified from IMPROVE PTFE filters. Further work to determine the stability and

592   ability to measure these compounds in aerosol mixtures as found in ambient samples is needed

593   before confidently using FT-IR on IMPROVE samples to measure organic sulfur compounds.

594   **5 Data Availability**

595   Data is available at https://doi.org/$10.25338/B8BH14$ (Anunciado et al., 2023).

596   **6 Author Contributions**

597   Conceptualization: AMD, TD; Formal Analysis:  MBA, TD, ST, AMD; Funding: AMD, TD;

598   Investigation: MBA, MDeB, LH, KL; Project Administration: AMD; Supervision: AMD, TD;

599   Writing First Draft:  MBA, TD; Writing Revisions and Editing: MBA, ST, TD, MDeB, LH, KL

600   AMD; software: ST, MA; Visualization: MA

601

602   **7 Competing Interests**

603   The contact author has declared that none of the authors has any competing interests.

604

605   **8 Acknowledgements**

606   AMD and MA wish to acknowledge funding from Research Triangle Institute (Agreement No.

607   62997) and the Interagency Monitoring of Protected Visual Environments (Grant No.

608   P21AC11294).  The authors would like to acknowledge Jason Surratt and his team for providing

609   the 2-MTS compound used in this study.

## 9 References

Spectral Database for Organic Compounds,SDBS: https://sdbs.db.aist.go.jp/sdbs/cgi-bin/direct_frame_top.cgi, last access: 22 February 2022.

Allen, A. G., Dick, A. L., and Davison, B. M.: Sources of atmospheric methanesulphonate, non-sea-salt sulphate, nitrate and related species over the temperate South Pacific, Atmospheric Environment, 31, 191–205, https://doi.org/10.1016/1352-2310(96)00194-X, 1997.

Allen, A. G., Davison, B. M., James, J. D., Robertson, L., Harrison, R. M., and Hewitt, C. N.: Influence of Transport over a Mountain Ridge on the Chemical Composition of Marine Aerosols during the ACE-2 Hillcloud Experiment, Journal of Atmospheric Chemistry, 41, 83–107, https://doi.org/10.1023/A:1013868729960, 2002.

Amore, A., Giardi, F., Becagli, S., Caiazzo, L., Mazzola, M., Severi, M., and Traversi, R.: Source apportionment of sulphate in the High Arctic by a 10 yr-long record from Gruvebadet Observatory (Ny-Ålesund, Svalbard Islands), Atmospheric Environment, 270, 118890, https://doi.org/10.1016/j.atmosenv.2021.118890, 2022.

Aneja, V. P. and Cooper, W. J.: Biogenic Sulfur Emissions, in: Biogenic Sulfur in the Environment, vol. 393, American Chemical Society, 2–13, https://doi.org/10.1021/bk-1989-0393.ch001, 1989.

Barnes, I., Becker, K. H., and Mihalopoulos, N.: An FTIR product study of the photooxidation of dimethyl disulfide, Journal of Atmospheric Chemistry, 18, 267–289, https://doi.org/10.1007/BF00696783, 1994.

Bates, T. S., Lamb, B. K., Guenther, A., Dignon, J., and Stoiber, R. E.: Sulfur emissions to the atmosphere from natural sources, Journal of Atmospheric Chemistry, 14, 315–337, https://doi.org/10.1007/BF00115242, 1992.

Becagli, S., Lazzara, L., Fani, F., Marchese, C., Traversi, R., Severi, M., di Sarra, A., Sferlazzo, D., Piacentino, S., Bommarito, C., Dayan, U., and Udisti, R.: Relationship between methanesulfonate (MS−) in atmospheric particulate and remotely sensed phytoplankton activity in oligo-mesotrophic central Mediterranean Sea, Atmospheric Environment, 79, 681–688, https://doi.org/10.1016/j.atmosenv.2013.07.032, 2013.

Boer, G. J., Sokolik, I. N., and Martin, S. T.: Infrared optical constants of aqueous sulfate–nitrate–ammonium multi-component tropospheric aerosols from attenuated total reflectance measurements—Part I: Results and analysis of spectral absorbing features, Journal of Quantitative Spectroscopy and Radiative Transfer, 108, 17–38, https://doi.org/10.1016/j.jqsrt.2007.02.017, 2007.

Bondy, A. L., Craig, R. L., Zhang, Z., Gold, A., Surratt, J. D., and Ault, A. P.: Isoprene-Derived Organosulfates: Vibrational Mode Analysis by Raman Spectroscopy, Acidity-Dependent Spectral Modes, and Observation in Individual Atmospheric Particles, The Journal of Physical Chemistry A, 122, 303–315, https://doi.org/10.1021/acs.jpca.7b10587, 2018.

Boris, A. J., Takahama, S., Weakley, A. T., Debus, B. M., Fredrickson, C. D., Esparza-Sanchez, M., Burki, C., Reggente, M., Shaw, S. L., Edgerton, E. S., and Dillner, A. M.: Quantifying organic matter and functional groups in particulate matter filter samples from the southeastern United States – Part 1: Methods,

647    Atmospheric Measurement Techniques, 12, 5391–5415, https://doi.org/10.5194/amt-12-5391-2019,
648    2019.

649    Boris, A. J., Takahama, S., Weakley, A. T., Debus, B. M., Shaw, S. L., Edgerton, E. S., Joo, T., Ng, N. L., and
650    Dillner, A. M.: Quantifying organic matter and functional groups in particulate matter filter samples from
651    the southeastern United States – Part 2: Spatiotemporal trends, Atmospheric Measurement Techniques,
652    14, 4355–4374, https://doi.org/10.5194/amt-14-4355-2021, 2021.

653    Campbell, J. R., Battaglia, M. Jr., Dingilian, K., Cesler-Maloney, M., St Clair, J. M., Hanisco, T. F., Robinson,
654    E., DeCarlo, P., Simpson, W., Nenes, A., Weber, R. J., and Mao, J.: Source and Chemistry of
655    Hydroxymethanesulfonate (HMS) in Fairbanks, Alaska, Environmental Science & Technology, 56, 7657–
656    7667, https://doi.org/10.1021/acs.est.2c00410, 2022.

657    Chackalackal, S. M. and Stafford, F. E.: Infrared Spectra of Methane-, Fluoro-, and Chlorosulfonic Acids,
658    Journal of the American Chemical Society, 88, 4815–4819, https://doi.org/10.1021/ja00973a010, 1966.

659    Chapman, E. G., Barinaga, C. J., Udseth, H. R., and Smith, R. D.: Confirmation and quantitation of
660    hydroxymethanesulfonate in precipitation by electrospray ionization-tandem mass spectrometry,
661    Atmospheric Environment. Part A. General Topics, 24, 2951–2957, https://doi.org/10.1016/0960-
662    1686(90)90475-3, 1990.

663    Chen, C., Zhang, Z., Wei, L., Qiu, Y., Xu, W., Song, S., Sun, J., Li, Z., Chen, Y., Ma, N., Xu, W., Pan, X., Fu, P.,
664    and Sun, Y.: The importance of hydroxymethanesulfonate (HMS) in winter haze episodes in North China
665    Plain, Environmental Research, 211, 113093, https://doi.org/10.1016/j.envres.2022.113093, 2022.

666    Chen, Y., Zhang, Y., Lambe, A. T., Xu, R., Lei, Z., Olson, N. E., Zhang, Z., Szalkowski, T., Cui, T., Vizuete, W.,
667    Gold, A., Turpin, B. J., Ault, A. P., Chan, M. N., and Surratt, J. D.: Heterogeneous Hydroxyl Radical
668    Oxidation of Isoprene-Epoxydiol-Derived Methyltetrol Sulfates: Plausible Formation Mechanisms of
669    Previously Unexplained Organosulfates in Ambient Fine Aerosols, Environmental Science & Technology
670    Letters, https://doi.org/10.1021/acs.estlett.0c00276, 2020.

671    Chen, Y., Dombek, T., Hand, J., Zhang, Z., Gold, A., Ault, A. P., Levine, K. E., and Surratt, J. D.: Seasonal
672    Contribution of Isoprene-Derived Organosulfates to Total Water-Soluble Fine Particulate Organic Sulfur
673    in the United States, ACS Earth and Space Chemistry, 5, 2419–2432,
674    https://doi.org/10.1021/acsearthspacechem.1c00102, 2021.

675    Chihara, G.: Measurement of Infrared Absorption Spectra by Absorption on Japanese Hand-made Paper
676    and Its Application to Paper Chromatography., Chemical & Pharmaceutical Bulletin, 6, 143–147,
677    https://doi.org/10.1248/cpb.6.143, 1958.

678    Debus, B., Takahama, S., Weakley, A. T., Seibert, K., and Dillner, A. M.: Long-Term Strategy for Assessing
679    Carbonaceous Particulate Matter Concentrations from Multiple Fourier Transform Infrared (FT-IR)
680    Instruments: Influence of Spectral Dissimilarities on Multivariate Calibration Performance, Applied
681    Spectroscopy, 73, 271–283, https://doi.org/10.1177/0003702818804574, 2019.

682    Debus, B., Weakley, A. T., Takahama, S., George, K. M., Amiri-Farahani, A., Schichtel, B., Copeland, S.,
683    Wexler, A. S., and Dillner, A. M.: Quantification of major particulate matter species from a single filter
684    type using infrared spectroscopy – application to a large-scale monitoring network, Atmospheric
685    Measurement Techniques, 15, 2685–2702, https://doi.org/10.5194/amt-15-2685-2022, 2022.

686    Decesari, S., Facchini, M. C., Fuzzi, S., and Tagliavini, E.: Characterization of water-soluble organic
687    compounds in atmospheric aerosol: A new approach, Journal of Geophysical Research: Atmospheres,
688    105, 1481–1489, https://doi.org/10.1029/1999JD900950, 2000.

689    Dovrou, E., Lim, C. Y., Canagaratna, M. R., Kroll, J. H., Worsnop, D. R., and Keutsch, F. N.: Measurement
690    techniques for identifying and quantifying hydroxymethanesulfonate (HMS) in an aqueous matrix and
691    particulate matter using aerosol mass spectrometry and ion chromatography, Atmospheric
692    Measurement Techniques, 12, 5303–5315, https://doi.org/10.5194/amt-12-5303-2019, 2019.

693    Fankhauser, A. M., Lei, Z., Daley, K. R., Xiao, Y., Zhang, Z., Gold, A., Ault, B. S., Surratt, J. D., and Ault, A.
694    P.: Acidity-Dependent Atmospheric Organosulfate Structures and Spectra: Exploration of Protonation
695    State Effects via Raman and Infrared Spectroscopies Combined with Density Functional Theory, The
696    Journal of Physical Chemistry A, 126, 5974–5984, https://doi.org/10.1021/acs.jpca.2c04548, 2022.

697    Frossard, A. A., Shaw, P. M., Russell, L. M., Kroll, J. H., Canagaratna, M. R., Worsnop, D. R., Quinn, P. K.,
698    and Bates, T. S.: Springtime Arctic haze contributions of submicron organic particles from European and
699    Asian combustion sources, Journal of Geophysical Research: Atmospheres, 116,
700    https://doi.org/10.1029/2010JD015178, 2011.

701    von Glasow, R. and Crutzen, P. J.: Model study of multiphase DMS oxidation with a focus on halogens,
702    Atmospheric Chemistry and Physics, 4, 589–608, https://doi.org/10.5194/acp-4-589-2004, 2004.

703    Grübler, A.: A Review of Global and Regional Sulfur Emission Scenarios, Mitigation and Adaptation
704    Strategies for Global Change, 3, 383–418, https://doi.org/10.1023/A:1009651624257, 1998.

705    Hansen, A. M. K., Kristensen, K., Nguyen, Q. T., Zare, A., Cozzi, F., Nøjgaard, J. K., Skov, H., Brandt, J.,
706    Christensen, J. H., Ström, J., Tunved, P., Krejci, R., and Glasius, M.: Organosulfates and organic acids in
707    Arctic aerosols: speciation, annual variation and concentration levels, Atmospheric Chemistry & Physics,
708    14, 7807–7823, https://doi.org/10.5194/acp-14-7807-2014, 2014.

709    Harrill, A. J.: Aqueous-Phase Processing of 2-Methyltetrol Sulfates by Hydroxyl Radical Oxidation in Fog
710    and Cloud Water Mimics:  Implications for Isoprene-Derived Secondary Organic Aerosol, 2020.

711    Hawkins, L. N., Russell, L. M., Covert, D. S., Quinn, P. K., and Bates, T. S.: Carboxylic acids, sulfates, and
712    organosulfates in processed continental organic aerosol over the southeast Pacific Ocean during
713    VOCALS-REx 2008, Journal of Geophysical Research: Atmospheres, 115,
714    https://doi.org/10.1029/2009JD013276, 2010.

715    Hettiyadura, A. P. S., Stone, E. A., Kundu, S., Baker, Z., Geddes, E., Richards, K., and Humphry, T.:
716    Determination of atmospheric organosulfates using HILIC chromatography with MS detection,
717    Atmospheric Measurement Techniques, 8, 2347–2358, https://doi.org/10.5194/amt-8-2347-2015, 2015.

718    Hettiyadura, A. P. S., Jayarathne, T., Baumann, K., Goldstein, A. H., de Gouw, J. A., Koss, A., Keutsch, F.
719    N., Skog, K., and Stone, E. A.: Qualitative and quantitative analysis of atmospheric organosulfates in
720    Centreville, Alabama, Atmospheric Chemistry and Physics, 17, 1343–1359, https://doi.org/10.5194/acp-
721    17-1343-2017, 2017.

722 Hoffmann, E. H., Tilgner, A., Schrödner, R., Bräuer, P., Wolke, R., and Herrmann, H.: An advanced
723 modeling study on the impacts and atmospheric implications of multiphase dimethyl sulfide chemistry,
724 Proceedings of the National Academy of Sciences, 113, 11776–11781, 2016.

725 Kamruzzaman, M., Takahama, S., and Dillner, A. M.: Quantification of amine functional groups and their
726 influence on OM/OC in the IMPROVE network, Atmospheric Environment, 172, 124–132,
727 https://doi.org/10.1016/j.atmosenv.2017.10.053, 2018.

728 Knovel - Yaws' Critical Property Data for Chemical Engineers and Chemists - Table 12. Vapor Pressure -
729 Organic Compounds, log P = A - B/(T + C):
730 https://app.knovel.com/kn/resources/kt009ZN2S3/kpYCPDCECD/eptble/itable?b-
731 =&columns=1%2C2%2C3%2C6%2C4%2C5%2C10%2C11%2C13%2C14%2C12%2C7%2C8%2C9, last
732 access: 7 September 2022.

733 Krost, K. J. and McClenny, W. A.: FT-IR Transmission Spectroscopy for Quantitation of Ammonium
734 Bisulfate in Fine-Particulate Matter Collected on Teflon® Filters, Applied Spectroscopy, 48, 702–705,
735 1994.

736 Kuzmiakova, A., Dillner, A. M., and Takahama, S.: An automated baseline correction protocol for infrared
737 spectra of atmospheric aerosols collected on polytetrafluoroethylene (Teflon) filters, Atmospheric
738 Measurement Techniques, 9, 2615–2631, https://doi.org/10.5194/amt-9-2615-2016, 2016.

739 Kwong, K. C., Chim, M. M., Hoffmann, E. H., Tilgner, A., Herrmann, H., Davies, J. F., Wilson, K. R., and
740 Chan, M. N.: Chemical Transformation of Methanesulfonic Acid and Sodium Methanesulfonate through
741 Heterogeneous OH Oxidation, ACS Earth and Space Chemistry, 2, 895–903,
742 https://doi.org/10.1021/acsearthspacechem.8b00072, 2018a.

743 Kwong, K. C., Chim, M. M., Davies, J. F., Wilson, K. R., and Chan, M. N.: Importance of sulfate radical
744 anion formation and chemistry in heterogeneous OH oxidation of sodium methyl sulfate, the smallest
745 organosulfate, Atmospheric Chemistry and Physics (Online), 18, https://doi.org/10.5194/acp-18-2809-
746 2018, 2018b.

747 Larkin, P. J.: Chapter 6 - IR and Raman Spectra–Structure Correlations: Characteristic Group Frequencies,
748 in: Infrared and Raman Spectroscopy (Second Edition), edited by: Larkin, P. J., Elsevier, 85–134,
749 https://doi.org/10.1016/B978-0-12-804162-8.00006-9, 2018.

750 Laurent, J.-P. and Allen, D. T.: Size Distributions of Organic Functional Groups in Ambient Aerosol
751 Collected in Houston, Texas Special Issue of *Aerosol Science and Technology* on Findings from the Fine
752 Particulate Matter Supersites Program, Aerosol Science and Technology, 38, 82–91,
753 https://doi.org/10.1080/02786820390229561, 2004.

754 Lee, J.-K., Lee, J.-S., Ahn, Y.-S., and Kang, G.-H.: Restoring the Reactivity of Organic Acid Solution Used for
755 Silver Recovery from Solar Cells by Fractional Distillation, Sustainability, 11, 3659,
756 https://doi.org/10.3390/su11133659, 2019.

757 Lee, S.-H., Murphy, D. M., Thomson, D. S., and Middlebrook, A. M.: Nitrate and oxidized organic ions in
758 single particle mass spectra during the 1999 Atlanta Supersite Project, Journal of Geophysical Research:
759 Atmospheres, 108, SOS 5-1-SOS 5-8, https://doi.org/10.1029/2001JD001455, 2003.

760  Lin-Vien, D., Colthup, N. B., Fateley, W. G., and Grasselli, J. G.: CHAPTER 14 - Organic Sulfur Compounds,
761  in: The Handbook of Infrared and Raman Characteristic Frequencies of Organic Molecules, edited by:
762  Lin-Vien, D., Colthup, N. B., Fateley, W. G., and Grasselli, J. G., Academic Press, San Diego, 225–250,
763  https://doi.org/10.1016/B978-0-08-057116-4.50020-1, 1991.

764  Liu, S., Takahama, S., Russell, L. M., Gilardoni, S., and Baumgardner, D.: Oxygenated organic functional
765  groups and their sources in single and submicron organic particles in MILAGRO 2006 campaign,
766  Atmospheric Chemistry & Physics, 9, 6849–6863, https://doi.org/10.5194/acp-9-6849-2009, 2009.

767  Liu, S., Ahlm, L., Day, D. A., Russell, L. M., Zhao, Y., Gentner, D. R., Weber, R. J., Goldstein, A. H., Jaoui,
768  M., Offenberg, J. H., Kleindienst, T. E., Rubitschun, C., Surratt, J. D., Sheesley, R. J., and Scheller, S.:
769  Secondary organic aerosol formation from fossil fuel sources contribute majority of summertime organic
770  mass at Bakersfield, Journal of Geophysical Research: Atmospheres, 117,
771  https://doi.org/10.1029/2012JD018170, 2012.

772  Lloyd, A. G. and Dodgson, K. S.: Infrared studies on sulphate esters. II. Monosaccharide sulphates,
773  Biochim Biophys Acta, 46, 116–120, https://doi.org/10.1016/0006-3002(61)90653-9, 1961.

774  Lloyd, A. G., Dodgson, K. S., Price, R. G., and Rose, F. A.: Infrared studies on sulphate esters. I.
775  Polysaccharide sulphates, Biochim Biophys Acta, 46, 108–115, https://doi.org/10.1016/0006-
776  3002(61)90652-7, 1961.

777  Ma, T., Furutani, H., Duan, F., Kimoto, T., Jiang, J., Zhang, Q., Xu, X., Wang, Y., Gao, J., Geng, G., Li, M.,
778  Song, S., Ma, Y., Che, F., Wang, J., Zhu, L., Huang, T., Toyoda, M., and He, K.: Contribution of
779  hydroxymethanesulfonate (HMS) to severe winter haze in the North China Plain, Atmospheric Chemistry
780  and Physics, 20, 5887–5897, https://doi.org/10.5194/acp-20-5887-2020, 2020.

781  Moch, J. M., Dovrou, E., Mickley, L. J., Keutsch, F. N., Cheng, Y., Jacob, D. J., Jiang, J., Li, M., Munger, J.
782  W., Qiao, X., and Zhang, Q.: Contribution of Hydroxymethane Sulfonate to Ambient Particulate Matter: A
783  Potential Explanation for High Particulate Sulfur During Severe Winter Haze in Beijing, Geophysical
784  Research Letters, 45, 11,969-11,979, https://doi.org/10.1029/2018GL079309, 2018.

785  Moch, J. M., Dovrou, E., Mickley, L. J., Keutsch, F. N., Liu, Z., Wang, Y., Dombek, T. L., Kuwata, M.,
786  Budisulistiorini, S. H., Yang, L., Decesari, S., Paglione, M., Alexander, B., Shao, J., Munger, J. W., and
787  Jacob, D. J.: Global Importance of Hydroxymethanesulfonate in Ambient Particulate Matter: Implications
788  for Air Quality, Journal of Geophysical Research: Atmospheres, 125, e2020JD032706,
789  https://doi.org/10.1029/2020JD032706, 2020.

790  Okabayashi, H., Okuyama, M., Kitagawa, T., and Miyazawa, T.: The Raman Spectra and Molecular
791  Conformations of Surfactants in Aqueous Solution and Crystalline States, Bulletin of the Chemical
792  Society of Japan, 47, 1075–1077, https://doi.org/10.1246/bcsj.47.1075, 1974.

793  Olson, C. N., Galloway, M. M., Yu, G., Hedman, C. J., Lockett, M. R., Yoon, T., Stone, E. A., Smith, L. M.,
794  and Keutsch, F. N.: Hydroxycarboxylic Acid-Derived Organosulfates: Synthesis, Stability, and
795  Quantification in Ambient Aerosol, Environmental Science & Technology, 45, 6468–6474,
796  https://doi.org/10.1021/es201039p, 2011.

797  Pavia, D. L., Lampman, G. M., Kriz, G. S., and Vyvyan, J. A.: Introduction to Spectroscopy, Cengage
798  Learning, 745 pp., 2008.

799    Peng, C. and Chan, C. K.: The water cycles of water-soluble organic salts of atmospheric importance,
800    Atmospheric Environment, 35, 1183–1192, https://doi.org/10.1016/S1352-2310(00)00426-X, 2001.

801    Reggente, M., Höhn, R., and Takahama, S.: An open platform for Aerosol InfraRed Spectroscopy analysis
802    – AIRSpec, Atmospheric Measurement Techniques, 12, 2313–2329, https://doi.org/10.5194/amt-12-
803    2313-2019, 2019.

804    Russell, L. M., Bahadur, R., and Ziemann, P. J.: Identifying organic aerosol sources by comparing
805    functional group composition in chamber and atmospheric particles, Proceedings of the National
806    Academy of Sciences, 108, 3516–3521, https://doi.org/10.1073/pnas.1006461108, 2011.

807    Ruthenburg, T. C., Perlin, P. C., Liu, V., McDade, C. E., and Dillner, A. M.: Determination of organic matter
808    and organic matter to organic carbon ratios by infrared spectroscopy with application to selected sites in
809    the IMPROVE network, Atmospheric Environment, 86, 47–57,
810    https://doi.org/10.1016/j.atmosenv.2013.12.034, 2014.

811    Saltzman, E. S., Savoie, D. L., Prospero, J. M., and Zika, R. G.: Methanesulfonic acid and non-sea-salt
812    sulfate in pacific air: Regional and seasonal variations, Journal of Atmospheric Chemistry, 4, 227–240,
813    https://doi.org/10.1007/BF00052002, 1986.

814    Sato, S., Higuchi, S., and Tanaka, S.: Structural Examinations of "Sodium FormaldehydeSulfoxylate" by
815    Infrared and Raman Spectroscopy, Nippon Kagaku Kaishi, 1984, 1151–1157,
816    https://doi.org/10.1246/nikkashi.1984.1151, 1984.

817    Segneanu, A. E., Gozescu, I., Dabici, A., Sfirloaga, P., and Szabadai, Z.: Organic Compounds FT-IR
818    Spectroscopy, IntechOpen, https://doi.org/10.5772/50183, 2012.

819    Seinfeld, J. H. and Pandis, S. N.: Atmospheric Chemistry and Physics: From Air Pollution to Climate
820    Change, Wiley, 2016.

821    Shurvell, H. F.: Spectra– Structure Correlations in the Mid- and Far-Infrared, in: Handbook of Vibrational
822    Spectroscopy, American Cancer Society, https://doi.org/10.1002/0470027320.s4101, 2006.

823    Smith, S. J., van Aardenne, J., Klimont, Z., Andres, R. J., Volke, A., and Delgado Arias, S.: Anthropogenic
824    sulfur dioxide emissions: 1850–2005, Atmospheric Chemistry and Physics, 11, 1101–1116,
825    https://doi.org/10.5194/acp-11-1101-2011, 2011.

826    Song, S., Gao, M., Xu, W., Sun, Y., Worsnop, D. R., Jayne, J. T., Zhang, Y., Zhu, L., Li, M., Zhou, Z., Cheng,
827    C., Lv, Y., Wang, Y., Peng, W., Xu, X., Lin, N., Wang, Y., Wang, S., Munger, J. W., Jacob, D. J., and McElroy,
828    M. B.: Possible heterogeneous chemistry of hydroxymethanesulfonate (HMS) in northern China winter
829    haze, Atmospheric Chemistry and Physics, 19, 1357–1371, https://doi.org/10.5194/acp-19-1357-2019,
830    2019.

831    Stone, E. A., Yang, L., Yu, L. E., and Rupakheti, M.: Characterization of organosulfates in atmospheric
832    aerosols at Four Asian locations, Atmospheric Environment, 47, 323–329,
833    https://doi.org/10.1016/j.atmosenv.2011.10.058, 2012.

834    Surratt, J. D., Chan, A. W. H., Eddingsaas, N. C., Chan, M., Loza, C. L., Kwan, A. J., Hersey, S. P., Flagan, R.
835    C., Wennberg, P. O., and Seinfeld, J. H.: Reactive intermediates revealed in secondary organic aerosol

836    formation from isoprene, Proceedings of the National Academy of Sciences, 107, 6640–6645,
837    https://doi.org/10.1073/pnas.0911114107, 2010.

838    Tang, K.: Chemical Diversity and Biochemical Transformation of Biogenic Organic Sulfur in the Ocean,
839    Frontiers in Marine Science, 7, 2020.

840    U.S. EPA. Comptox Chemicals Dashboard:
841    https://comptox.epa.gov/dashboard/chemical/details/DTXSID80805075 (accessed November 14, 2022)
842    Methyl 10,10-diethoxydec-2-ene-4,6,8-triynoate, 2022.

843    Wang, Y., Zhao, Y., Wang, Y., Yu, J.-Z., Shao, J., Liu, P., Zhu, W., Cheng, Z., Li, Z., Yan, N., and Xiao, H.:
844    Organosulfates in atmospheric aerosols in Shanghai, China: seasonal and interannual variability, origin,
845    and formation mechanisms, Atmospheric Chemistry and Physics, 21, 2959–2980,
846    https://doi.org/10.5194/acp-21-2959-2021, 2021.

847    Wei, L., Fu, P., Chen, X., An, N., Yue, S., Ren, H., Zhao, W., Xie, Q., Sun, Y., Zhu, Q.-F., Wang, Z., and Feng,
848    Y.-Q.: Quantitative Determination of Hydroxymethanesulfonate (HMS) Using Ion Chromatography and
849    UHPLC-LTQ-Orbitrap Mass Spectrometry: A Missing Source of Sulfur during Haze Episodes in Beijing,
850    Environmental Science & Technology Letters, 7, 701–707, https://doi.org/10.1021/acs.estlett.0c00528,
851    2020.

852    Yazdani, A., Dudani, N., Takahama, S., Bertrand, A., Prévôt, A. S. H., El Haddad, I., and Dillner, A. M.:
853    Fragment ion–functional group relationships in organic aerosols using aerosol mass spectrometry and
854    mid-infrared spectroscopy, Atmospheric Measurement Techniques, 15, 2857–2874,
855    https://doi.org/10.5194/amt-15-2857-2022, 2022.

856    Zawadowicz, M. A., Proud, S. R., Seppalainen, S. S., and Cziczo, D. J.: Hygroscopic and phase separation
857    properties of ammonium sulfate/organics/water ternary solutions, Atmospheric Chemistry and Physics,
858    15, 8975–8986, https://doi.org/10.5194/acp-15-8975-2015, 2015.

859    Zeng, G., Kelley, J., Kish, J. D., and Liu, Y.: Temperature-Dependent Deliquescent and Efflorescent
860    Properties of Methanesulfonate Sodium Studied by ATR-FTIR Spectroscopy, The Journal of Physical
861    Chemistry A, 118, 583–591, https://doi.org/10.1021/jp405896y, 2014.

862    Zhao, X., Shi, X., Ma, X., Zuo, C., Wang, H., Xu, F., Sun, Y., and Zhang, Q.: 2-Methyltetrol sulfate ester-
863    initiated nucleation mechanism enhanced by common nucleation precursors: A theory study, Science of
864    The Total Environment, 723, 137987, https://doi.org/10.1016/j.scitotenv.2020.137987, 2020.

865    Zhong, L. and Parker, S. F.: Structure and vibrational spectroscopy of methanesulfonic acid, Royal Society
866    of Open Science, 5, 181363, https://doi.org/10.1098/rsos.181363, 2022.

867